

# Synthesis, Photophysics, and Electroluminescence of Mesogen-Jacketed 2D Conjugated Copolymers Based on Fluorene–Thiophene–Oxadiazole Derivative

Qian Yang, Hao Jin, Yiding Xu, Ping Wang, Xiaochao Liang, Zhihao Shen,\*  
Xiaofang Chen, Dechun Zou, Xinghe Fan,\* and Qifeng Zhou\*

Beijing National Laboratory for Molecular Sciences, Key Laboratory of Polymer Chemistry and Physics of Ministry of Education, College of Chemistry and Molecular Engineering, Peking University, Beijing 100871, China

Received October 28, 2008; Revised Manuscript Received December 15, 2008

**ABSTRACT:** A novel monomer 3-{2,5-bis[(4-hexadecyloxy-phenyl)-1,3,4-oxadiazole]phenyl}-2,5-dibromothiophene (MJTO) was copolymerized with 9,9'-dioctylfluorene to generate a series of new conjugated copolymers (PFT0.1, PFT0.5, PFT1, PFT5, PFT10, PFT25, and PFT50) by Suzuki coupling reaction. They were characterized by molecular weight determination,  $^1\text{H}$  NMR, elemental analysis, TGA, DSC, UV–vis absorption, emission spectroscopy, and cyclic voltammetry. The copolymers exhibited high decomposition temperatures reaching 417 °C and high  $T_g$  values reaching 145 °C. The photophysical properties were greatly influenced by the content of the MJTO monomer. The copolymers in solution and film states of PFT25 and PFT50 showed two distinct absorption peaks corresponding to absorptions from the electron-transport side chain and the hole-transport backbone, respectively, instead of a single peak when MJTO content was below 10.79%. The copolymers in solution with MJTO content below 10.79% shared similar emission spectra, whereas PFT25 and PFT50 showed absolutely different emission that red-shifted a lot. In the film state, the emission spectra gradually red-shifted when the MJTO content increased. The HOMO and LUMO energy levels were both lower than those of PF, which resulted in better electron injection and transport but still blue-green emission. Light-emitting diode devices were fabricated with a configuration of ITO/PEDOT–PSS/polymer/Ca (20 nm)/Al (70 nm) for all polymers. Among those devices, PFT5 attained brightness of 5558  $\text{cd}/\text{m}^2$  and current efficiency of 0.39  $\text{cd}/\text{A}$ , which proved that the introduction of a proper ratio of the novel thiophene–oxadiazole comonomer to PF could largely improve its EL properties.

## Introduction

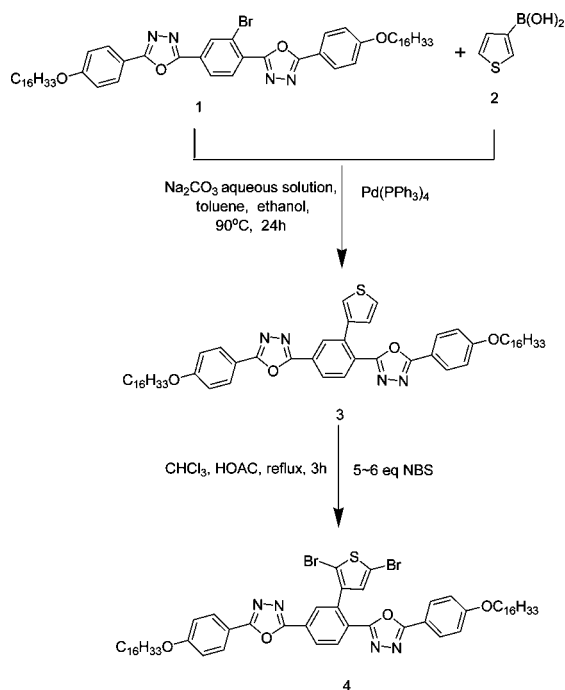
The development of polymers that possess both high performance and easy processability has become the major driving force for advanced lightweight polymeric light-emitting diodes (PLEDs). Conjugated polymers have received considerable attention because of their high heat-resistance, excellent dimensional stability, adjustable emitting color, and good compatibility with other polymers. Several main-chain conjugated polymers have been developed to be used in the field of PLEDs, such as poly(*p*-phenylene vinylene) (PPV),<sup>1</sup> poly(*p*-phenylene) (PPP),<sup>2</sup> polythiophene (PT),<sup>3</sup> polyfluorene (PF),<sup>4</sup> their copolymers, and their soluble derivatives. Although the electroluminescence properties of main-chain conjugated polymers are much better than those of side-chain conjugated polymers, there still remains a lot of tough work in improving device properties, including low turn-on voltage, high color purity, high luminance, and high efficiency. To reach these goals, much more work is needed to search for better molecular structure and explore the structure–property relationships of polymers, especially between the molecular structure and electroluminescence properties. PF and its derivatives are among the most widely studied blue-light emitting polymers because of their high photoluminescence quantum efficiencies and facile color tunability. However, their tendency to form ketonic defects or long-wavelength excimers in the solid state leads to their poor spectral stability. In general, there are two strategies for suppressing the less efficient and red-shifted excimer emission: (1) introducing a small amount of low-bandgap chromophores and bulky side chains to the PF backbones and (2) copolymerizing with other suitable mono-

mers. For the second approach, it is much more attractive to utilize thiophene-based comonomer because of the versatility in its structure modification as well as its good semiconducting property. Tsui et al. synthesized soluble fluorene copolymers with thiophene or bithiophene through Stille cross-coupling reaction and investigated their redox and electrochromic properties.<sup>5</sup> Liu et al. and Pal et al. independently prepared soluble alternating conjugated copolymers composed of 9,9-dihexylfluorene and substituted bithiophene or thiophene moieties by palladium-catalyzed Suzuki coupling reaction and studied the influence of the substitution on the electronic properties.<sup>6,7</sup> Lim et al. reported the syntheses of PF alternating copolymers containing a thiophene-condensed thieno[3,2-*b*]thiophene moiety via a palladium-catalyzed Suzuki coupling reaction with the maximum luminance in light-emitting diode device of 970  $\text{cd}/\text{m}^2$ .<sup>8</sup> They also discussed the potential application in organic field-effect transistor (OFET).<sup>9</sup> Tang et al. studied fluorene-thieno[3,2-*b*]thiophene-conjugated copolymers for applications in light-emitting diodes and photovoltaic cells and also simulated the optimized geometries of polymer chains to evaluate the effect of different substitution positions by using density functional theory.<sup>10</sup>

To obtain highly efficient light-emitting devices, a balance in the injection and transportation of both holes and electrons into the polymer emissive layer is necessary. Because PF and PT are both electron-rich and hole-transport, it is necessary to introduce electron-withdrawing units to the main chains or side chains to attain large electron affinities. 5-Diphenyl-1,3,4-oxadiazole (OXD) derivatives are the most widely used electron-injection and hole-blocking materials because 1,3,4-OXD moieties possess many advantages, such as prominent electron affinity, high photoluminescence quantum yields, and good thermal and chemical stability.<sup>11–13</sup> The low-molecular-weight

\* To whom the correspondence should be addressed. E-mail: fanxh@pku.edu.cn; zshen@pku.edu.cn; qfzhou@pku.edu.cn.

Scheme 1. Synthesis of Monomer 4



compounds,<sup>14–16</sup> dendritic,<sup>17</sup> and polymeric derivatives<sup>18–21</sup> containing OXD units have already been investigated. Some PFs containing OXD units have been synthesized and reported recently, and different attachment manners of the OXD unit have been explored to study their influence on the EL properties. For instance, Sung et al. synthesized soluble fluorene-based alternating copolymers containing symmetrical and asymmetrical OXD pendants with different terminal groups by the palladium-catalyzed Suzuki coupling reaction, and they proved that effective energy transfer from the OXD pendants to the conjugated polymer backbones had occurred, and the polymers with asymmetrical OXD pendants had better properties than those with symmetrical OXD units.<sup>22</sup> Wu et al. synthesized OXD-containing PF copolymers (PF-OXD) by the attachment of two OXD groups to the C-9 position of the alternating fluorene unit to obtain a 3D cardo structure, and they prepared a double-layer LED device using this polymer as the emitting layer with high brightness of 2770 cd/m<sup>2</sup>.<sup>23</sup>

The previous work in our group indicated that the bulky and waist-attaching mesogen-jacketed structure adopted in our research could enhance the performance of EL devices of the side-chain conjugated polymers containing OXD units.<sup>24,25</sup> Because main-chain conjugated polymers possess much better performance than side-chain conjugated polymers,

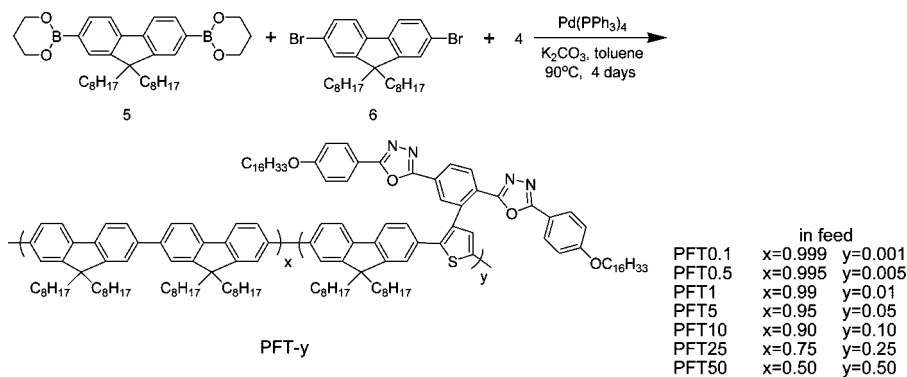
if we introduce such bulky and waist-attaching jacketed structure to the PF backbone, then much better performance can be expected. Therefore, we employ this jacketed structure in the copolymers of fluorene–thiophene derivatives to reduce the interactions within and between the backbones of PFs and tune the optical properties of the target copolymers. The fluorene–thiophene-conjugated copolymers reported before were mostly comprised of flexible side chains in the three position of thiophene and bithiophene or thieno[3,2-*b*]thiophene in main chains. The research of such a structure with a rigid electron-transport unit in the side chain to form a 2D conjugated system has not yet been reported. In this investigation, we designed and synthesized a series of mesogen-jacketed copolymers of fluorene and thiophene-based comonomers of different molar ratios via Suzuki cross-coupling reaction. The general properties of these copolymers, including thermal, optical, and electrochemical properties, are discussed. Furthermore, the potential application of these copolymers as active layers in PLEDs is investigated.

## Experimental Section

**Materials and Measurements.** All of the chemicals were purchased from Aldrich, Acros, and Alfa Aesar and were used without further purification. THF was heated under reflux over sodium/benzophenone and was freshly distilled before use. Toluene was heated under reflux over CaH<sub>2</sub> for at least 8 h and was distilled before use. The catalyst Pd(PPh<sub>3</sub>)<sub>4</sub> was synthesized according to the previously reported procedure.<sup>26</sup>

All new compounds were identified by <sup>1</sup>H NMR, mass spectroscopy, and elemental analysis (EA). The <sup>1</sup>H NMR spectra were recorded with a Bruker ARX400 spectrometer at room temperature with deuterated chloroform (CDCl<sub>3</sub>) as the solvent, and the chemical shifts were reported in ppm with tetramethylsilane (TMS) as the internal standard. Mass spectra were recorded on a Bruker Daltonics Autoflex III MALDI-TOF spectrometer. Elemental analysis was carried out on an Elementar Vario EL instrument. The molecular weight and molecular weight distribution of the polymers were determined by gel permeation chromatography (GPC) on a Waters 2410 instrument equipped with three Waters  $\mu$ -Styragel columns (10<sup>3</sup>, 10<sup>4</sup>, and 10<sup>5</sup> Å) in series, with THF as the eluent at a flow rate of 1.0 mL/min at 35 °C. Monodisperse polystyrene standards were used for calibration. The thermogravimetric analysis (TGA) of the polymers was performed under a nitrogen atmosphere at a heating rate of 10 °C/min with a TA SDT Q600 analyzer. The differential scanning calorimetry (DSC) examination was carried out on a TA DSC Q100 calorimeter with a programmed heating procedure in nitrogen. The sample size was about 5 mg, and it was encapsulated in hermetically sealed aluminum pans whose weights were kept constant. The temperature and heat flow scales at different cooling and heating rates were calibrated using standard materials such as indium and benzoic acid. The glass-transition temperatures (*T*<sub>g</sub>) were obtained from the second

Scheme 2. Synthesis of the Copolymers (PFT)



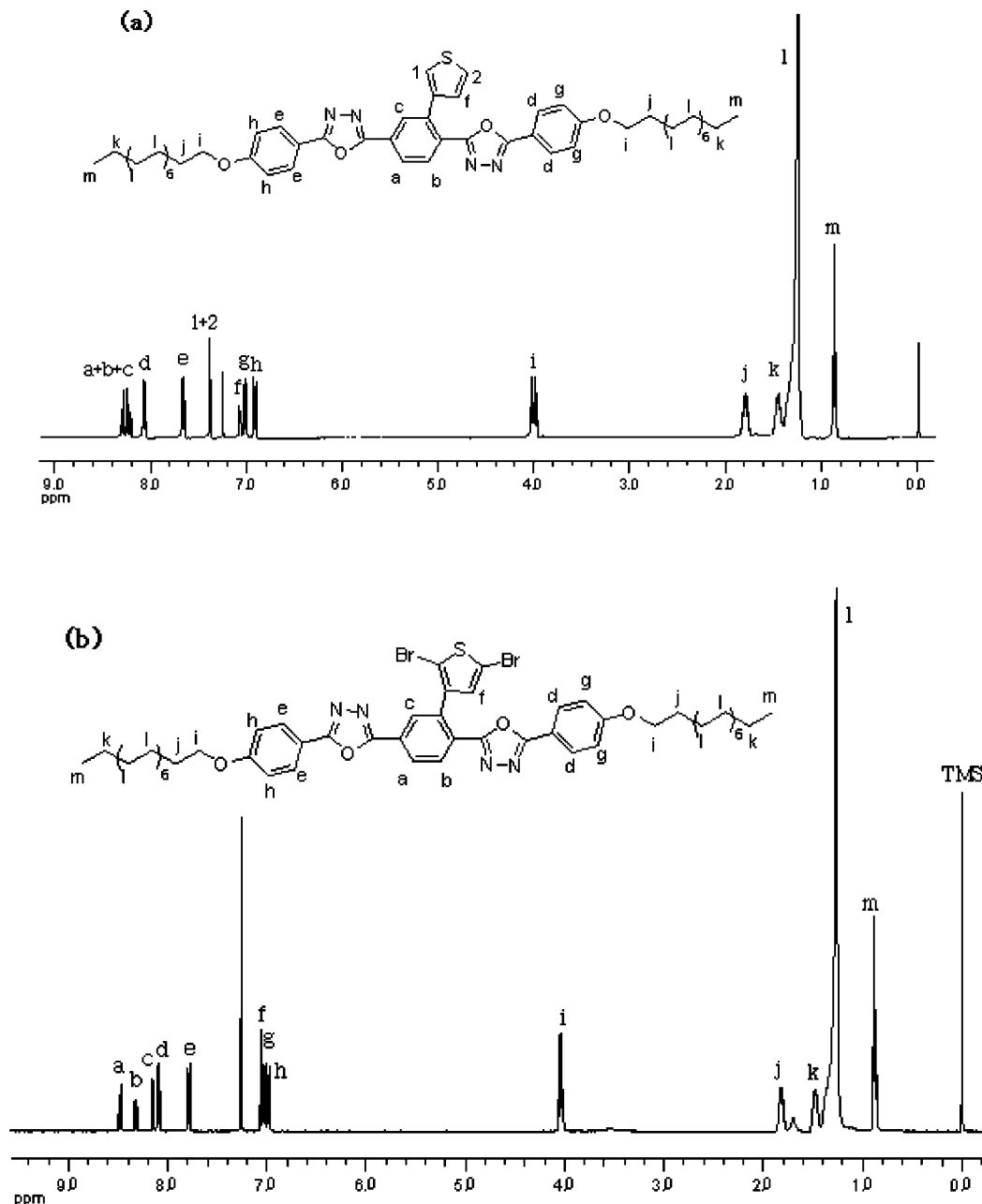


Figure 1.  $^1\text{H}$  NMR spectra of (a) compound 3 and (b) compound 4 in  $\text{CDCl}_3$ .

Table 1. Polymerization Results and Thermal Properties of the Copolymers

polymer	yield (%)	$M_n (\times 10^4)^a$	$M_w (\times 10^4)^a$	$\text{PDI}^a$	$T_d (\text{°C})^b$	$T_g (\text{°C})^c$
PF	46	1.14	2.07	1.82	416	54
PFT0.1	44	0.91	1.37	1.50	414	55
PFT0.5	44	1.21	1.88	1.55	398	59
PFT1	62	1.18	1.81	1.53	411	62
PFT5	64	1.33	1.64	1.23	417	67
PFT10	64	1.76	3.21	1.82	407	111
PFT25	62	1.51	2.66	1.76	413	136
PFT50	83	1.55	2.33	1.50	364	145

<sup>a</sup>  $M_n$ ,  $M_w$ , and PDI of the polymers were determined by GPC using polystyrene standards in THF solutions. <sup>b</sup> Temperature at 5 wt % loss under nitrogen atmosphere determined by TGA at a heating rate of 10  $^{\circ}\text{C}/\text{min}$ . <sup>c</sup> Glass-transition temperature determined by DSC in nitrogen in the second heating curve at a heating rate of 20  $^{\circ}\text{C}/\text{min}$ .

heating curve. Absorption spectra were measured with a Perkin-Elmer lambda 35 UV/vis spectrophotometer, and PL spectra were obtained using a Hitachi F-4500 fluorescence spectrophotometer.

The cyclic voltammograms were recorded with a voltammetric analyzer (model CHI630C from Shanghai Chenhua Instrument) in a solution of tetrabutylammonium perchlorate (0.1 M) in acetonitrile with a scanning rate of 100 mV/s at room temperature under a nitrogen atmosphere. The measuring cell consisted of vitreous carbon electrode as the working electrode, Ag/AgCl electrode as the reference electrode, and platinum wire electrode as the auxiliary electrode. The polymer films were coated on the working electrode by solution casting and were then dried in air. The energy levels were calculated with a ferrocene (FOC) value of  $-4.8$  eV with respect to vacuum level as a calibration reference. After CV measurements of polymers, two drops of FOC in acetonitrile (3 mM) were added and measured for calibration. Therefore, the HOMO level of the polymers could be calculated by the equation  $E_{\text{HOMO}} = -e (E_{\text{onset(ox)}} - E_{1/2,\text{FOC}}) - 4.8$  eV, and the LUMO level could be estimated by the equation  $E_{\text{LUMO}} = -e (E_{\text{onset(red)}} - E_{1/2,\text{FOC}}) - 4.8$  eV, where  $E_{1/2,\text{FOC}}$  stands for the half-wave potential of  $\text{Fc}/\text{Fc}^+$ .

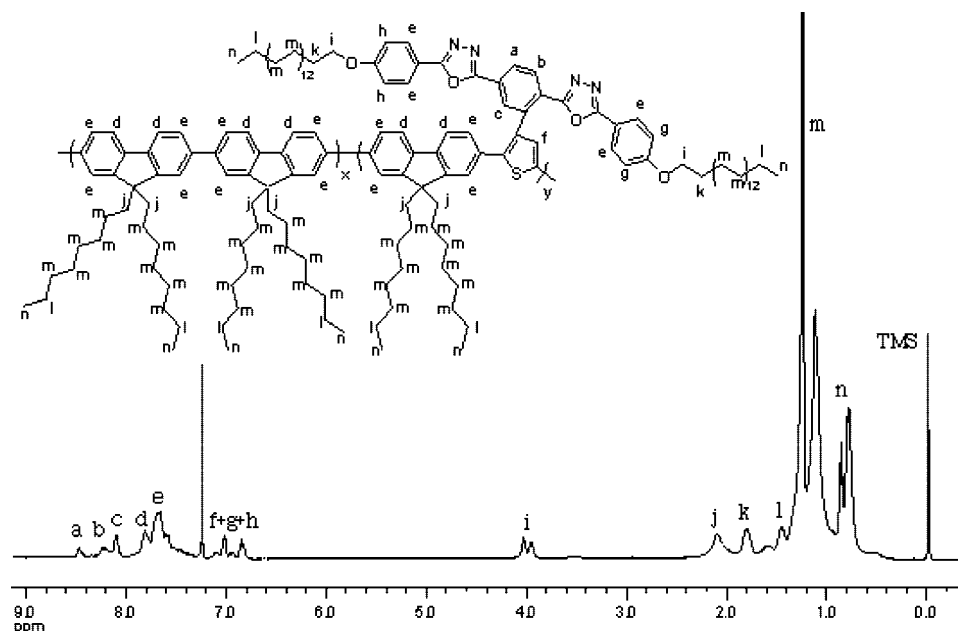


**Figure 2.** Estimation of copolymer compositions via  $^1\text{H}$  NMR spectra taking copolymer PFT25 as an example.

**Table 2.** Optical Properties of Copolymers in Chloroform Solutions and Solid Films

polymer	solution <sup>a</sup>			film <sup>b</sup>	
	absorption $\lambda_{\text{max}}$ (nm)	PL $\lambda_{\text{max}}$ (nm) <sup>c</sup>	$\phi_{\text{PL}}$ <sup>d</sup>	absorption $\lambda_{\text{max}}$ (nm)	PL $\lambda_{\text{max}}$ (nm) <sup>e</sup>
PF	378	418 (440, 474) <sup>e</sup>	1.19	376	420 (454)
PFT0.1	382	418 (440, 474)	1.39	379	420 (454)
PFT0.5	380	418 (440, 474)	1.28	378	(420) 454
PFT1	380	418 (440, 474)	1.19	382	454 (478)
PFT5	388	420 (442, 478)	0.30	383 (435)	475
PFT10	386	419 (441, 477)	0.12	385	480
PFT25	(345) 395	513	0.06	(352, 373) 394	480, 505
PFT50	335, 412	(477) 508	0.05	259, 341, 368, 422	480, 510

<sup>a</sup> In chloroform (1 mg/10 mL). <sup>b</sup> Films were spin-cast from toluene solutions. <sup>c</sup> Excitation wavelength was 380 nm. <sup>d</sup> Fluorescence quantum efficiencies were measured in chloroform relative to quinine sulfate ( $\phi_{\text{PL}} = 0.55$ ). <sup>e</sup> Data in parentheses are the wavelengths of shoulders and subpeaks.

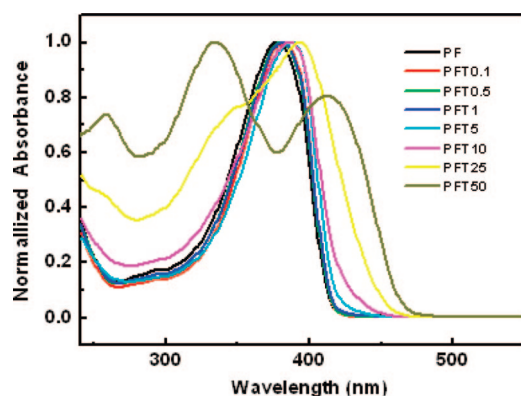


**Figure 3.** Normalized UV/vis absorption spectra of PF, PFT0.1, PFT0.5, PFT1, PFT5, PFT10, PFT25, and PFT50 (1 mg/10 mL) measured in chloroform solutions at room temperature.

**Synthesis of the Monomer (Scheme 1).** 2,5-Bis[(4-hexadecyloxy-phenyl)-1,3,4-oxadiazole]bromobenzene **1**. This compound was synthesized according to the previously reported procedure.<sup>27</sup>

3-[2,5-Bis[(4-hexadecyloxy-phenyl)-1,3,4-oxadiazole]phenyl]thiophene **3**. To a mixture of **1** (2.78 g, 3.00 mmol), thiophene-3-boronic acid (0.50 g, 3.90 mmol), and  $\text{Pd}(\text{PPh}_3)_4$  (0.12 g, 0.09 mmol) under an argon atmosphere were added toluene (60 mL), ethanol (30 mL),

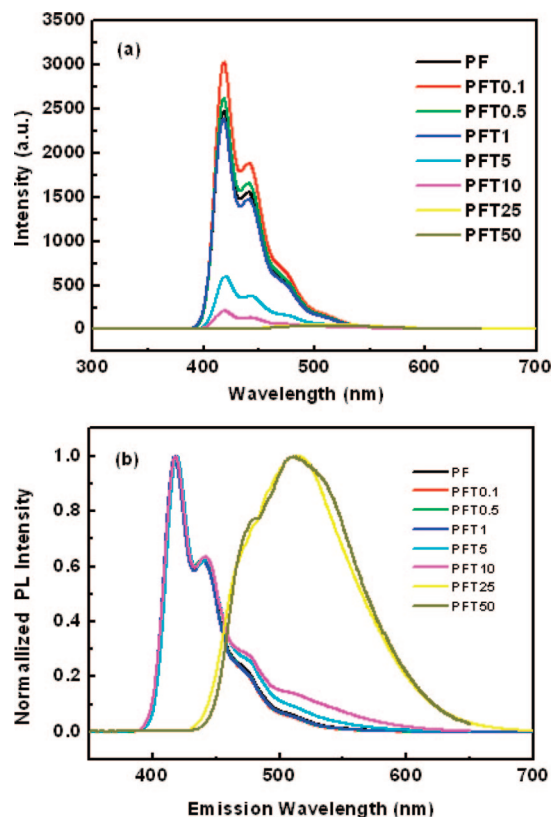


**Figure 4.** PL spectra (excitation: 380 nm) of PF, PFT0.1, PFT0.5, PFT1, PFT5, PFT10, PFT25, and PFT50 (1 mg/10 mL) in chloroform (a) before and (b) after normalization.

and  $\text{Na}_2\text{CO}_3$  aqueous solution (1 M, 60 mL) by a syringe in order. The reaction mixture was allowed to react at 90 °C for 24 h under vigorous stirring and was then filtered under reduced pressure and washed by  $\text{CH}_2\text{Cl}_2$  and water and neutralized. After extraction, the organic layer was washed with water and dried over anhydrous  $\text{MgSO}_4$ . After removing the drying agent and solvent in vacuo, the residue was subjected to column chromatography (silica gel) with  $\text{CH}_2\text{Cl}_2$ /ethyl acetate 10:1 (v/v) as eluant. Recrystallization of the obtained crude product from DMF gave the pure white product **3** (2.31 g, 82.9%).  $^1\text{H}$  NMR (400 MHz,  $\text{CDCl}_3$ ,  $\delta$ ): 8.26–8.33 (m,



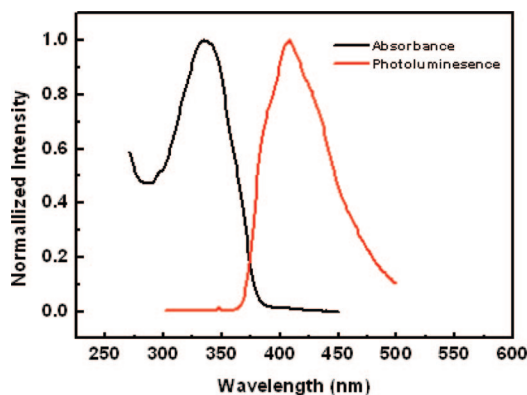


**Figure 5.** Normalized absorption and photoluminescence (excitation: 334 nm) spectra of MJTO monomer ( $1 \times 10^{-5}$  M) in chloroform.

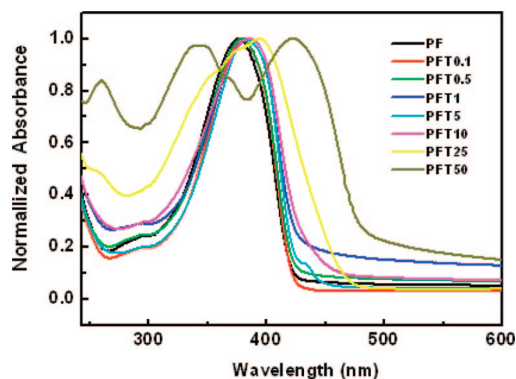


**Figure 6.** Normalized absorption spectra of PF, PFT0.1, PFT0.5, PFT1, PFT5, PFT10, PFT25, and PFT50 in the film state.

4H, phenyl-H), 8.08–8.11 (d, 2H, phenyl-H), 7.67–7.70 (d, 2H, phenyl-H), 7.39–7.40 (d, 2H, thiophene-H), 7.07–7.10 (t, 1H, thiophene-H), 7.02–7.05 (d, 2H, phenyl-H), 6.92–6.95 (d, 2H, phenyl-H), 3.98–4.07 (p, 4H,  $-\text{OCH}_2\text{CH}_2-$ ), 1.78–1.83 (m, 4H,  $-\text{CH}_2\text{CH}_2\text{CH}_2-$ ), 1.46 (m, 4H,  $-\text{CH}_2\text{CH}_2\text{CH}_2-$ ), 1.26 (m, 48H,  $-\text{CH}_2\text{CH}_2\text{CH}_2-$ ), 0.76–0.90 (t, 6H,  $-\text{CH}_3$ ). Anal. Calcd for  $\text{C}_{58}\text{H}_{80}\text{N}_4\text{O}_4\text{S}$ : C, 74.96; H, 8.68; N, 6.03. Found: C, 74.64; H, 9.02; N, 5.93. MS (MALDI)  $m/z$ : 929.7 (calcd for  $\text{C}_{58}\text{H}_{80}\text{N}_4\text{O}_4\text{S}$ , 929.4).

**3-[2,5-Bis[(4-hexadecyloxy-phenyl)-1,3,4-oxadiazole]phenyl]-2,5-dibromothiophene 4.** To a solution of **3** (1.21 g, 1.30 mmol) in the mixture of chloroform (30 mL) and acetic acid (30 mL), *N*-bromosuccinimide (1.16 g, 6.50 mmol) was added in portions over 30 min. After being stirred for 3 h under reflux, the mixture solution was poured in cold water, neutralized, and extracted with chloroform. The combined organic layers were dried over anhydrous  $\text{MgSO}_4$ . After the removal of the drying agent and solvent in vacuo, the residue was subjected to column chromatography (silica gel) with ethyl acetate/petrol ether 1:3 (v/v) as eluant. The product was obtained as a white solid with a yield of 0.25 g (17.7 %).  $^1\text{H}$  NMR (400 MHz,  $\text{CDCl}_3$ ,  $\delta$ ): 8.47–8.49 (d, 1H, phenyl-H), 8.30–8.34 (d, 2H, phenyl-H), 8.15 (s, 1H, phenyl-H), 8.08–8.11 (d, 2H, phenyl-H), 7.78–7.80 (d, 2H, phenyl-H), 7.06 (s, 1H, thiophene-H), 7.02–7.05 (d, 2H, phenyl-H), 6.97–7.00 (d, 2H, phenyl-H), 4.01–4.07 (t, 4H,  $-\text{OCH}_2\text{CH}_2-$ ), 1.82 (m, 4H,  $-\text{CH}_2\text{CH}_2\text{CH}_2-$ ), 1.48 (m, 4H,  $-\text{CH}_2\text{CH}_2\text{CH}_2-$ ), 1.26 (m, 48H,  $-\text{CH}_2\text{CH}_2\text{CH}_2-$ ), 0.86–0.90 (t, 6H,  $-\text{CH}_3$ ). Anal. Calcd for  $\text{C}_{58}\text{H}_{78}\text{Br}_2\text{N}_4\text{O}_4\text{S}$ : C, 64.08; H, 7.23; N, 5.15. Found: C, 63.95; H, 7.33; N, 5.07. MS (MALDI)  $m/z$ : 1087.5 (calcd for  $\text{C}_{58}\text{H}_{78}\text{Br}_2\text{N}_4\text{O}_4\text{S}$ , 1087.1).

**Polymer Synthesis (Scheme 2).** The synthesis of PF and copolymers (PFT0.1, PFT0.5, PFT1, PFT5, PFT10, PFT25, and PFT50) was carried out using the palladium-catalyzed Suzuki coupling reaction. Taking PFT25 as an example, the mixture of 9,9-dioctylfluorene-2,7-bis(trimethyleneborate) **5** (0.11 g, 0.20 mmol), 9,9-dioctyl-2,7-dibromofluorene **6** (0.05 g, 0.10 mmol), the MJTO monomer **4** (0.11 g, 0.10 mmol), and  $\text{Pd}(\text{PPh}_3)_4$  (0.01 g,

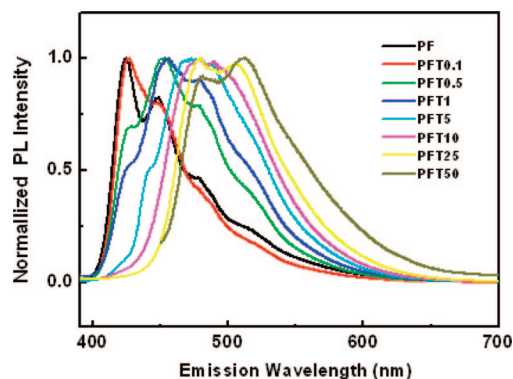


**Figure 7.** Normalized PL spectra of PF, PFT0.1, PFT0.5, PFT1, PFT5, PFT10, PFT25, and PFT50 in the film state (excitation wavelength: 380 nm).

0.01 mmol) was repeated to pump and purge with argon three times, and then toluene (5 mL), an aqueous solution of  $\text{K}_2\text{CO}_3$  (0.50 M, 5 mL), and ethanol (2 mL) were added. The mixture was allowed to react at 90 °C under vigorous stirring. After 4 days, **5** and 9,9-dioctyl-2-bromofluorene<sup>28</sup> were successively added with an interval of 8 h to end-cap the polymer chain. The whole mixture was dropped in a large excess of methanol. The resulting solid was collected by filtration and subjected to Soxhlet extraction with acetone to remove oligomers and catalyst residues (yield: 0.17 g, 61.9%).  $^1\text{H}$  NMR (400 MHz,  $\text{CDCl}_3$ ,  $\delta$ ): 8.48 (m, 2H, phenyl-H), 8.11–8.24 (m, 5H, phenyl-H), 7.62–7.83 (m, 19H, phenyl-H), 6.86–7.03 (m, 5H, phenyl-H, thiophene-H), 3.98–4.04 (m, 4H,  $-\text{OCH}_2\text{CH}_2-$ ), 2.11–2.18 (m, 9H,  $-\text{CH}_2\text{CH}_2\text{CH}_2-$ ), 1.81 (m, 6H,  $-\text{CH}_2\text{CH}_2\text{CH}_2-$ ), 1.46–1.57 (m, 5H,  $-\text{CH}_2\text{CH}_2\text{CH}_2-$ ), 1.14–1.26 (m, 112H,  $-\text{CH}_2\text{CH}_2\text{CH}_2-$ ), 0.80–0.88 (m, 34H,  $-\text{CH}_3$ ).

#### Fabrication of the Polymeric Light-Emitting Diode Devices.

Double-layer light-emitting diodes (ITO/PEDOT–PSS/polymer/Ca/Al) were fabricated for the investigation of optoelectronic characteristics. The patterned indium tin oxide (ITO) glass substrate was cleaned in turn with substrate-cleaning detergent, deionized water, acetone, and ethanol for 15 min under ultrasonic conditions and finally treated with UV–ozone for about 25 min. Then, a hole-injection layer of PEDOT/PSS was spin-coated on it at 4000 rpm with about 50 nm in thickness and was dried by baking in air at 120 °C for 3 h. Then, the emitting layer was spin-cast onto the PEDOT/PSS layer at a speed of 2000 rpm from toluene solution (10 mg/mL) through a 0.2  $\mu\text{m}$  Teflon filter, followed by drying overnight. Finally, the coated ITO was transferred to a deposition chamber with a base pressure of  $0.6 \times 10^{-4}$  Pa, and a layer of Ca and Al electrodes was vacuum-deposited on the polymer layer. The emitting area was  $2 \times 2 \text{ mm}^2$ . The EL spectra were measured with a spectrofluorometer FP-6200 (JASCO). A source-measure unit R6145 (Advantest), multimeter 2000 (Keithley), and luminance meter LS-110 (Minolta) were used for I–V–L measurements. Relative luminance was directly detected by the use of a multifunctional optical meter 1835-C (Newport). All fabrication and characterization of the light-emitting diode devices was performed in air and at room temperature without protective encapsulation.

#### Results and Discussion

**Synthesis and Characterization.** Synthetic routes employed for the preparation of the monomer and polymers are shown in Schemes 1 and 2, respectively. Compound **3** was prepared via Suzuki cross-coupling reaction. With recrystallization from DMF after purification with column chromatography, very pure compound can be conveniently obtained in a total yield of 82.9%. Because the thiophene ring is electron-rich, NBS can be used to brominate compound **3** with the polarity of reaction solvent increased. In this research, considering the large hindrance and relatively poor solubility of MJTO monomer, 5 to 6 equiv of NBS, which was fairly in excess, was added to

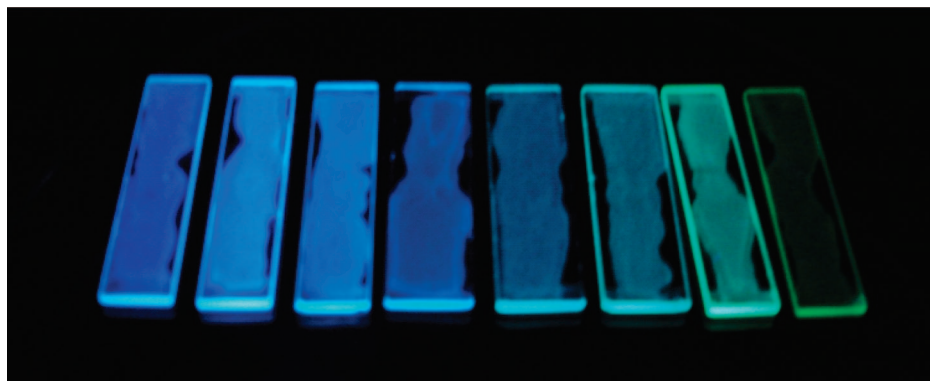


**Figure 8.** Photoluminescence of the polymers (PF, PFT0.1, PFT0.5, PFT1, PFT5, PFT10, PFT25, and PFT50 from left to right in turn) in film state under irradiation with UV lamp ( $\lambda = 365$  nm).

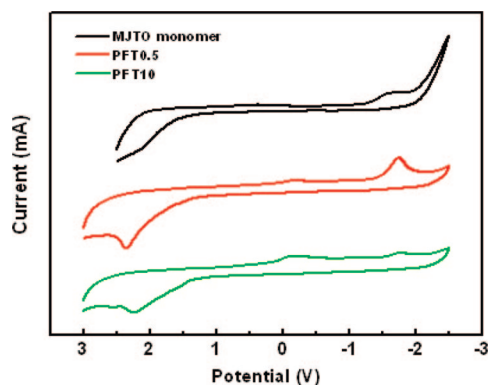


**Figure 9.** Typical cyclic voltammograms of films on a vitreous carbon electrode in 0.1 mol/L  $\text{Bu}_4\text{NClO}_4$ , acetonitrile solution.

the reaction system in portions, and a mixed solvent of  $\text{CHCl}_3$  and acetic acid (v/v 1:1) was employed. As a result of the rather poor solubility of MJTO monomer and its small polarity difference with compound **3** and the monobrominated product, the yield of pure dibrominated product after column chromatography was limited (17.7%), and the unseparated part and monobrominated part were combined and recycled. In the  $^1\text{H}$  NMR spectra (Figure 1), the peaks at chemical shifts of 7.39–7.40 (d, 2H) in Figure 1a completely disappeared in Figure 1b, so it can be concluded that compound **3** was successfully dibrominated into 2,5-dibromothiophene derivative with neither residual monobrominated product nor other product with unexpected substituted positions. The result of elemental analysis was in high agreement as well. We have also attempted to use compound **1** and 2,5-dibromo-thiophene-3-boronic acid to perform the Suzuki cross-coupling reaction, expecting to get the target MJTO monomer. Although many of efforts were made, it finally failed with no cross-coupling product.

The polymerization was also proceeded by the well-known palladium-catalyzed Suzuki coupling reaction between compound **5**, **6**, and functionalized MJTO monomer. The molar percentage of MJTO in the feed was between 0.1 and 50%, as shown in the numbers after PFT. The copolymers PFT0.1, PFT0.5, PFT1, PFT5, PFT10, PFT25, and PFT50 were soluble in common organic solvents such as chloroform, toluene, and dichloromethane. Their molecular weights were determined by GPC using monodisperse polystyrene as the calibration standard. As shown in Table 1, the weight-average molecular weights ( $M_w$ ) were  $(1.37\text{--}3.21) \times 10^4$  with polydispersity indexes (PDIs) around 1.23–1.82. The actual compositions of these copolymers were estimated from 400 MHz  $^1\text{H}$  NMR spectra (Figure 2). According to the ratio of the integral area of the peaks at 4.05 and 3.98 ppm corresponding to  $-\text{OCH}_2\text{CH}_2-$  of the terminal alkoxy versus that of the peak at 2.12 ppm

corresponding to  $-\text{CH}_2\text{CH}_2-$  of the 9-substituted alkyl, the actual compositions of the obtained copolymers were calculated. Anal. found for PFT5, 5.65%; for PFT10, 10.79%; for PFT25, 30.64%; and for PFT50, 69.92%. The content of MJTO monomer was so little in the copolymers PFT0.1, PFT0.5, and PFT1 that it did not show obvious peaks at 4 ppm, but it could be analogized that MJTO were effectively reacted into these three copolymers from the results of other copolymers with a larger content of MJTO. The molar percentages of MJTO monomer were greater than the feed compositions (0.1, 0.5, 1, 5, 10, 25, and 50 mol %), suggesting that the MJTO monomer exhibited a slightly higher reactivity than that of the 9,9-dioctyl-2,7-dibromofluorene **6**.

Thermal properties of the polymers were evaluated by TGA and DSC, and the results are summarized in Table 1. This series of copolymers had fairly high decomposition temperatures, with the highest of 417  $^\circ\text{C}$ , indicating that the copolymers were quite stable at elevated temperatures. The glass-transition temperatures ( $T_g$ ) of the polymers obtained by DSC were greatly influenced by the content of the rigid MJTO monomer. PFT0.1, PFT0.5, and PFT1 had glass-transition temperatures that were slightly higher than that of PF as a result of the low molar percentage of the MJTO monomer. The  $T_g$  values were 67  $^\circ\text{C}$  for PFT5, 111  $^\circ\text{C}$  for PFT10, 136  $^\circ\text{C}$  for PFT25, and 145  $^\circ\text{C}$  for PFT50, which were much higher than 54  $^\circ\text{C}$  for PF. It was obvious that the incorporation of MJTO largely increased the  $T_g$  value, which was possibly due to reduced segmental motions and large hindrance of the bulky side chains. A high  $T_g$  value is very important for this type of polymers when used as emissive materials in PLEDs.

**Photophysical Properties.** The photophysical characteristics of the copolymers were investigated both in  $\text{CHCl}_3$  and as films cast from toluene solutions. Their absorption and emission spectral data are summarized in Table 2. Figures 3 and 4 display the absorption and photoluminescence (PL) spectra of PF, PFTs (1 mg/10 mL), and MJTO in dilute solution ( $1 \times 10^{-5}$  M). PF and PFT0.1, PFT0.5, PFT1, PFT5, and PFT10 showed the major and maximum absorption in the range of 378–388 nm, which can be attributed to  $\pi-\pi^*$  transitions of the main-chain  $\pi$ -conjugated system. The absorption spectra exhibited a red shift with an increase in MJTO fraction, that is, from 378 nm for PF to 388 nm for PFT5 and 386 nm for PFT10. The red shift demonstrated that the  $\pi$ -conjugation in the backbone had not been interrupted after incorporating the MJTO unit similar to the work reported before.<sup>29</sup> Instead, the conjugation was enhanced. When the MJTO content was increased to 30.64 and 69.92% for PFT25 and PFT50, respectively, the absorption spectra exhibited two separate peaks at 345 and 395 nm and 335 and 412 nm, respectively. The relatively short wavelength absorption showed great resemblance to that of MJTO, so it

Table 3. Electrochemical Properties of the Copolymers

polymer	$\lambda_{\text{edge}}$ (nm) <sup>a</sup>	optical $E_g$ (eV) <sup>b</sup>	$E_{\text{ox}}^{\text{onset}}$ vs Ag/AgCl (V)	$E_{\text{red}}^{\text{onset}}$ vs Ag/AgCl (V)	$E_{\text{HOMO}}$ (eV)	$E_{\text{LUMO}}$ (eV)	electrochemical $E_g$ (eV) <sup>c</sup>
PF	419	2.96	1.35	−1.54	−5.77	−2.88	2.89
PFT0.1	420	2.95	1.78	−1.50	−6.18	−2.90	3.28
PFT0.5	422	2.94	1.82	−1.46	−6.20	−2.91	3.29
PFT1	424	2.92	1.69	−1.46	−6.15	−3.00	3.15
PFT5	444	2.79	1.36	−1.40	−5.78	−3.02	2.76
PFT10	430	2.88	1.41	−1.49	−5.81	−2.91	2.90
PFT25	462	2.68	1.76	−1.83	−6.19	−2.60	3.59
PFT50	479	2.59	1.80	−0.83	−6.17	−3.54	2.63

<sup>a</sup>  $\lambda_{\text{edge}}$  was the onset value of absorption spectrum in long wavelength range. <sup>b</sup> Optical band gap was obtained from the empirical formula  $E_g = 1240/\lambda_{\text{edge}}$  eV. <sup>c</sup> Electrochemical  $E_g = E_{\text{ox}}^{\text{onset}} - E_{\text{red}}^{\text{onset}}$  eV,  $E_{\text{HOMO}} = -e(E_{\text{ox}}^{\text{onset}} - E_{1/2,\text{FOC}}) - 4.8$  eV,  $E_{\text{LUMO}} = -e(E_{\text{red}}^{\text{onset}} - E_{1/2,\text{FOC}}) - 4.8$  eV.

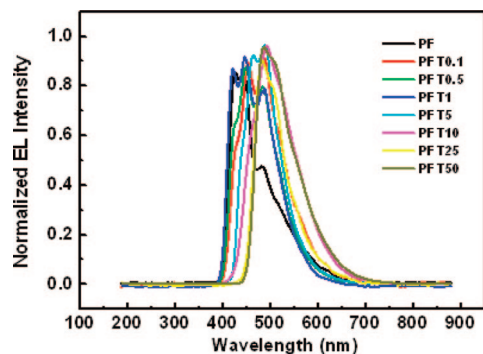


Figure 10. Normalized EL spectra of the devices (ITO/PEDOT-PSS/polymer/Ca/Al) at 8 V bias voltage.

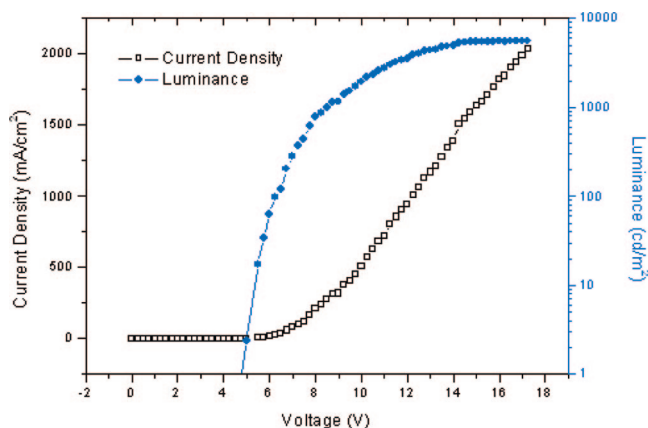


Figure 11. Current density-voltage and brightness-voltage characteristics of the EL device of copolymer PFT5.

corresponded to the absorption at 334 nm for the MJTO unit (Figure 5), whereas the relatively long wavelength absorption corresponded to the main-chain absorption and red-shifted 9 and 26 nm compared with PFT10. The phenomenon above indicated that when MJTO content was below 10.79%, the copolymers were similar to PF homopolymers slightly modified with the MJTO comonomer, whereas when the content of MJTO comonomer increased to 30.64 and 69.92%, the copolymers mainly acted as alternating copolymers between diboronester of dioctylfluorene and the MJTO comonomer. In general, the absorption spectra of this series of copolymers demonstrated that the side-chain oxadiazole unit could be effectively involved in the main-chain conjugation system and possessed a common localized  $\pi$ -system with the PF main chain when the molar ratio of MJTO monomer was below 10.79%. When the molar ratio of MJTO increased up to 30.64%, the copolymers exhibited absorptions that corresponded to the side chain and the main chain, respectively, so that there was an obvious shoulder in the absorption spectra of PFT25, and finally developed into two separated peaks when the content was up to 69.92%.

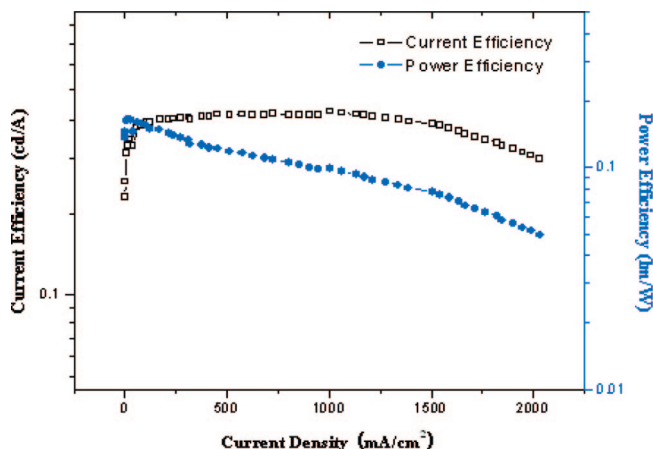


Figure 12. Current efficiency-current density and luminescence efficiency-current density characteristics of the EL device of copolymer PFT5.

Figure 4 shows the PL spectra of the polymers obtained in dilute chloroform solutions (excitation wavelength: 380 nm). The emission spectrum of PF exhibited typical vibronic progression with the 0–0 PL emission band situated at 418 nm, the 0–1 transition (vibronic bands) at 440 nm, and 0–2 transition at 474 nm.<sup>30</sup> The copolymers PFT0.1, PFT0.5, PFT1, PFT5, and PFT10 also displayed these three characteristic emission bands at about 418 to 420, 440 to 442, and 474 to 478 nm, and PFT0.1, PFT0.5, and PFT1 had almost the same photoluminescence spectra as those of PF. In addition, they all exhibited small shoulders at approximately 510 nm, corresponding to the unexpected green emission. With the MJTO content increasing to 5.65 and 10.79%, the relative intensity of the 0–2 transition shoulder at 478 nm and green emission at 510 nm became larger. For PFT25 and PFT50, the typical vibronic peaks of PF disappeared; instead, the peaks at 513 and 508 nm developed, which corresponded to the new original emission of PFT25 and PFT50 copolymers. Therefore, it was concluded that when the MJTO content was in the range of 1 to 10.79%, the copolymer chain tended to exhibit similar emissions to that of PF homopolymers, whereas when the content of MJTO increased to 30.64 and 69.92%, the copolymers had totally new emissions that were different from those of PF. The photoluminescence quantum efficiencies of the polymers (PF, PFT0.1, PFT0.5, PFT1, PFT5, PFT10, PFT25, and PFT50) using quinine sulfate as the reference, were 1.19, 1.39, 1.28, 1.19, 0.30, 0.12, 0.06, and 0.05 (Table 2), respectively, and they obviously reduced with increasing MJTO content. The PL spectral intensity strongly depended on the MJTO content, and the intensity gradually became smaller with increasing MJTO content (Figure 4a). Greatly reduced absorption of PFT25 and PFT50 at 380 nm (excitation wavelength) may lead to a decrease in its PL intensity, too, and the concentration quenching effect between MJTO moieties should also be considered.<sup>31</sup> The spectrum did not show any obvious blue shift, which indicated that the



Table 4. Electroluminescence Properties of the Devices

polymer	$V_{on}$ (V) <sup>a</sup>	$L_{max}$ (cd/m <sup>2</sup> ) <sup>b</sup>	emission wavelength ( $\lambda_{em}$ , nm) <sup>c</sup>	current efficiency (cd/A) <sup>d</sup>	luminescence efficiency (lm/W) <sup>e</sup>	(x,y) <sup>f</sup>	EQE (%)
PF	5.7	1009	426, 443, 481	0.13	0.043	(0.18, 0.16)	0.101
PFT0.1	5.6	2179	454, 487	0.26	0.090	(0.18, 0.23)	0.152
PFT0.5	4.8	1952	448, 483	0.05	0.018	(0.17, 0.19)	0.038
PFT1	5.8	874	422, 446, 484	0.14	0.003	(0.16, 0.17)	0.011
PFT5	4.8	5558	464, 489	0.39	0.165	(0.16, 0.24)	0.224
PFT10	4.5	1731	493	0.10	0.049	(0.22, 0.37)	0.043
PFT25	5.0	1588	482	0.18	0.073	(0.19, 0.40)	0.076
PFT50	6.6	384	487	0.11	0.037	(0.25, 0.46)	0.047

<sup>a</sup> Turn-on voltage at 1 cd/m<sup>2</sup>. <sup>b</sup> Maximum luminance. <sup>c</sup> Emission wavelength at the bias voltage of 8 V. <sup>d</sup> Maximum current efficiency. <sup>e</sup> Maximum luminescence efficiency. <sup>f</sup> 1931 CIE coordinate.

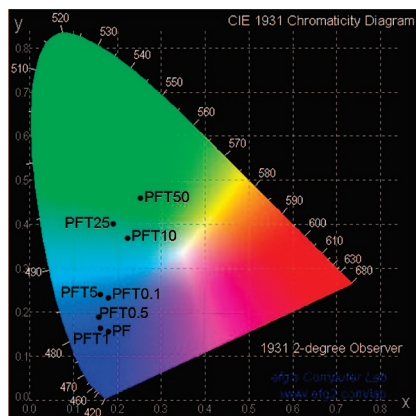


Figure 13. CIE 1931 chromaticity coordinates (x,y) of the devices of the PFTs.

attachment of the bulky jacketed oxadiazole side chains to the backbone did not make the main chain twist to decrease the effective conjugation length.<sup>32</sup>

Figures 6 and 7 show the absorption and PL spectra in the film state. The absorption spectra in the film state were similar to those in solution (Figure 3), and no obvious red shift was worth noticing except that the PFT5 film showed a small shoulder at longer wavelength, which may induce smaller band gap. As shown in Figure 7, the PL spectra of the copolymers red-shifted gradually and regularly as the MJTO content increased. Starting from emission at 420 and 454 nm of PF, the spectrum of PFT0.1 widened, but it could be clearly recognized as two distinguished peaks at the same emitting position as that of PF. PFT0.5 and PFT1 still had these peaks but showed great red shift, and the relative intensities of the three peaks or shoulders at 420, 454, and 478 nm changed a lot. PFT5 and PFT10 mainly emitted a single broad peak, which indicated the existence of effective exciton migration or energy transfer in the film state. However, for PFT25 and PFT50, the spectra separated into two different peaks again, and their positions were kept consistent with the spectra in solution in spite of 2 to 3 nm red shifts. The red-shift trend of these copolymers with increasing MJTO content could be seen clearly in the photographs (Figure 8) taken under irradiation with a UV lamp ( $\lambda = 365$  nm).

**Electrochemical Properties.** Cyclic voltammetry (CV) has been considered to be an effective method for investigating electrochemical properties of conjugated compounds. From the onset oxidation and reduction potentials in the cyclic voltammogram, the highest occupied molecular orbital (HOMO) and lowest unoccupied molecular orbital (LUMO) levels can be readily estimated, which correspond to ionization potential (IP) and electron affinity (EA), respectively. Polymer-coated vitreous carbon electrode was used as the working electrode in 0.10 M tetrabutylammonium perchlorate ( $\text{Bu}_4\text{NClO}_4$ ) in chromatographic grade acetonitrile. Typical cyclic voltammograms of

MJTO monomer, PFT0.5, and PFT10 in anodic and cathodic scans are shown as examples in Figure 9 with all related electrochemical data summarized in Table 3. The onset oxidation potentials were situated at 1.57 V for the MJTO monomer, 1.35 V for PF, and 1.36 to 1.82 V for PFT0.1, PFT0.5, PFT1, PFT5, PFT10, PFT25, and PFT50, from which their HOMO levels were estimated to be  $-5.93$ ,  $-5.77$ , and  $-5.78$  to  $-6.20$  eV, respectively, according to the equation  $\text{IP} = -e(E_{\text{onset(ox)}} - E_{1/2,\text{FOC}}) - 4.8$  eV. The onset reduction potentials of MJTO monomer, PF, PFT0.1, PFT0.5, PFT1, PFT5, PFT10, PFT25, and PFT50 were  $-1.28$ ,  $-1.54$ , and in the range of  $-1.83$  to  $-0.83$  V, with their LUMO levels estimated to be  $-3.08$ ,  $-2.88$ , and  $-3.54$  to  $-2.60$  eV according to the equation  $\text{EA} = -e(E_{\text{onset(red)}} - E_{1/2,\text{FOC}}) - 4.8$  eV. From the HOMO and LUMO levels, the band gaps of the MJTO monomer, PF, and the copolymers were estimated to be 2.85, 2.89, 3.28, 3.29, 3.15, 2.76, 2.90, 3.59, and 2.63 eV, respectively. The results showed that all of the copolymers had similar HOMO levels ( $-6.20$  to  $-6.15$  eV), except for PFT5 of  $-5.78$  eV and PFT10 of  $-5.81$  eV, which indicated that the incorporation of the MJTO monomer made the oxidation more difficult to be started. The LUMO energy levels of the copolymers were also lower, with exception for PFT25 of  $-2.60$  eV, and the lowest LUMO energy level was  $-3.54$  eV for PFT50. It indicated that the high electron affinity of the OXD unit was helpful in lowering the LUMO energy level, resulting in facilitated electron injection. The decrease in LUMO was smaller than that in HOMO, so most of the band gaps of the copolymers were larger than PF. The electrochemical band gaps were larger than optical band gaps because of the interface barrier for charge injection, which was in agreement with the previous reports.<sup>30</sup> Among the data of PFT copolymers, PFT5 had a much lower LUMO energy level and almost the same HOMO energy level as those of PF, which may result in the undermentioned best EL properties among these series of copolymers.

**Electroluminescence Properties of Polymeric Light-Emitting Diode Devices.** We fabricated double-layer electroluminescence devices with the configuration of ITO/PEDOT-PSS/polymer/Ca (20 nm)/Al (70 nm) to investigate their optoelectronic characteristics. Figure 10 shows the EL spectra of the devices. The major emission peak of the PF device was situated at 426 nm, which red-shifted 8 nm relative to that in the PL spectra. The strong minor peak and shoulder at 443 and 481 nm corresponded to the 0–1 and 0–2 vibronic transitions, respectively. For PFT1, the three characteristic peaks of PF also appeared, with almost no red shift compared with those of PF. The EL spectra of other copolymers gradually changed. In the EL spectra of PFT0.1 and PFT0.5, for instance, the emission at about 420 nm vanished, leaving two vibronic peaks at (448–454) nm and (483–487) nm, which was a little red-shifted with comparison with that of PF. PFT5 showed a spectrum that was similar to those of PFT0.1 and PFT0.5 with more red shifts. When the MJTO content further increased, the EL emission



spectra tended to be a single peak. For example, PFT10 exhibited a peak at 493 nm in its spectrum, and PFT25 and PFT50 both showed single peaks at 482 and 487 nm, respectively, located in the blue-emitting region, although the spectra of PFT25 and PFT50 revealed a trend of the growth of a shoulder situated at approximately 508 nm corresponding to the green emission. The trend of the EL spectra of PFT copolymers was similar to that observed in their PL spectra.

Figures 11 and 12 show the spectra of brightness and current density versus bias voltage and the spectra of current efficiency and luminescence efficiency versus current density of the EL device of PFT5, and the related characteristic data of all EL devices are summarized in Table 4. The turn-on voltages of the EL devices were in the range of 4.5 to 6.6 V, and the maximal brightness and current efficiency were 384–5558 cd/m<sup>2</sup> and 0.05 to 0.39 cd/A, respectively. The luminescence efficiency of the EL devices was (0.003 to 0.165) lm/W. In general, PFT5 exhibited the best property, which started to emit at a turn-on voltage of 4.8 V and had the highest brightness of 5558 cd/m<sup>2</sup>. Its current efficiency and luminescence efficiency were 0.39 cd/A and 0.165 lm/W, respectively, which possessed better properties than those of the similar previously reported work.<sup>29</sup> The maximal brightness of most of the devices surpassed that of the PF device (1009 cd/m<sup>2</sup>, 0.13 cd/A), for instance, PFT0.1 (2179 cd/m<sup>2</sup>, 0.26 cd/A), PFT0.5 (1952 cd/m<sup>2</sup>, 0.05 cd/A), PFT5, PFT10 (1731 cd/m<sup>2</sup>, 0.10 cd/A), and PFT25 (1588 cd/m<sup>2</sup>, 0.18 cd/A). It is worth noticing that the current efficiencies and luminescence efficiencies of PFT0.1 and PFT5 are relatively higher than those of the other copolymers, which could be induced by the more balanced carrier mobility. As is well known, the improvement of EL efficiencies depends on the balance of the two carriers, that is, electron and hole in transportation. If the quantities or the mobility of electrons and holes are not matched, then these two carriers would combine at a position other than the emission layer of the EL device, so the EL efficiencies would decrease abruptly. PFT0.1 and PFT5 probably reached better charge balance and easier transportation between different layers of the EL devices corresponding to their energy levels demonstrated above. In addition, there was no relatively large excess of the electron-affinitive OXD groups in the copolymers to act as electron traps to imbalance the charge transport as PFT50 did. In summary, the copolymers of PFT0.1 and PFT5 had a better balance of electron and hole mobility, so they represented relatively better current and luminescence efficiencies. The emitting color changed from blue to green as the MJTO content increased, as shown in Figure 13. In general, with an increase in MJTO content, the properties of the devices first improved until PFT5, which reached the maximum, and then gradually decreased, which indicated that the introduction of 5.65 mol % of the MJTO monomer could improve the EL properties of PF most notably and 5.65 mol % was the turning point.

## Conclusions

We have described the synthesis and characterization of new conjugated copolymers composed of 9,9-dioctylfluorene and novel thiophene-based monomer containing oxadiazole unit, and their potential application in PLED is discussed. The polymers were characterized by thermal analysis, optical spectroscopy, cyclic voltammetry, and electroluminescence analysis. The resulting polymers possessed good thermal stability, high glass-transition temperatures, and excellent solubility in common organic solvents. Their absorption spectra in solution and film state were similar, except for a little red shift in film state. The absorption spectra showed a single peak when the MJTO content was below 10.79% and gradually separated into two distinct absorption peaks that corresponded to the side-chain oxadiazole

unit and the backbone, respectively. The photoluminescence spectra in solution of copolymers with MJTO content below 10.79% were similar to those of PF, which indicates that they were mainly similar to PF homopolymers that were slightly modified with the MJTO comonomer. In particular, copolymers with MJTO content of <1% attained the same spectra as that of PF, whereas as the MJTO content increased to 5.65 and 10.79%, the intensity of the long wavelength emission was gradually enhanced. When the MJTO content increased to 30.64 and 69.92%, there were only long wavelength emissions in the spectra, which was the original emission of the copolymers that acted like alternating copolymers between diboronester of dioctylfluorene and the MJTO comonomer. In addition, the PL spectra in the film state exhibited a gradual shift to long wavelength when the MJTO content increased. The copolymers showed lower LUMO energy levels than that of PF, which indicated effective improvement of electron injection and transportation. The HOMO energy levels were also mostly lower, which made the emission of the copolymers still lying in the blue-green region. Electroluminescence was studied with the device configuration of ITO/PEDOT–PSS/polymer/Ca (20 nm)/Al (70 nm). The maximum brightness and current efficiency reached 5558 cd/m<sup>2</sup> and 0.39 cd/A, which was attained by the copolymer PFT5. It proved that the introduction of a proper ratio of the novel thiophene-based comonomer to PF could greatly improve its EL property.

**Acknowledgment.** The work described in this Article was supported by the National Science Foundation of China (grant nos.: 20634010, 20574002, 20874002, and 20874003).

## References and Notes

- (1) (a) Gustafsson, G.; Cao, Y.; Treacy, G. M.; Klavetter, F.; Colaneri, N.; Heeger, A. J. *Nature* **1992**, *357*, 477. (b) Greenham, N. C.; Moratti, S. C.; Bradley, D. D. C.; Friend, R. H.; Holmes, A. B. *Nature* **1993**, *365*, 628.
- (2) (a) Grem, G.; Leditzky, G.; Ullrich, B.; Leising, G. *Adv. Mater.* **1992**, *4*, 36. (b) Tour, J. M. *Adv. Mater.* **1994**, *6*, 190.
- (3) (a) Roncali, J. *Chem. Rev.* **1997**, *97*, 173. (b) Perepichka, I. F.; Perepichka, D. F.; Meng, H.; Wudl, F. *Adv. Mater.* **2005**, *17*, 2281.
- (4) (a) Pei, Q.; Yang, Y. *J. Am. Chem. Soc.* **1996**, *118*, 7416. (b) Grell, M.; Bradley, D. D. C.; Inbasekaran, M.; Woo, E. P. *Adv. Mater.* **1997**, *9*, 798. (c) Kim, J. S.; Friend, R. H.; Cacialli, F. *Appl. Phys. Lett.* **1999**, *74*, 3084. (d) Jenekhe, S. A.; Osaheni, J. A. *Science* **1994**, *265*, 765.
- (5) Tsui, B.; Reddinger, J. L.; Sotzing, G. A.; Soloducho, J.; Katritzky, A. R.; Reynolds, J. R. *J. Mater. Chem.* **1999**, *9*, 2189.
- (6) Liu, B.; Yu, W.-L.; Lai, Y.-H.; Huang, W. *Macromolecules* **2000**, *33*, 8945.
- (7) Pal, B.; Yen, W. C.; Yang, J. S.; Su, W. F. *Macromolecules* **2007**, *40*, 8189.
- (8) Lim, E.; Jung, B.-J.; Shim, H.-K. *Macromolecules* **2003**, *36*, 4288.
- (9) Lim, E.; Jung, B.-J.; Lee, J.; Shim, H.-K.; Lee, J.-I.; Yang, Y. S.; Do, L.-M. *Macromolecules* **2005**, *38*, 4531.
- (10) Tang, W. H.; Ke, L.; Tan, L. W.; Lin, T. T.; Kietzke, T.; Chen, Z. K. *Macromolecules* **2007**, *40*, 6164.
- (11) Adachi, C.; Tsutsui, T.; Saito, S. *Appl. Phys. Lett.* **1989**, *55*, 1489.
- (12) Kraft, A.; Grimsdale, A. C.; Holmes, A. B. *Angew. Chem., Int. Ed.* **1998**, *37*, 402.
- (13) Mitschke, U.; Bäuerle, P. *J. Mater. Chem.* **2000**, *10*, 1471.
- (14) Hughes, G.; Bryce, M. R. *J. Mater. Chem.* **2005**, *15*, 94.
- (15) Adachi, C.; Tokito, S.; Tsutsui, T.; Saito, S. *Jpn. J. Appl. Phys.* **1988**, *27*, L713.
- (16) Wang, C.; Jung, G.-Y.; Batsanov, A. S.; Bryce, M. R.; Petty, M. C. *J. Mater. Chem.* **2002**, *12*, 173.
- (17) Chien, Y.-Y.; Wong, K.-T.; Chou, P.-T.; Cheng, Y.-M. *Chem. Commun.* **2002**, 2874.
- (18) Cha, S. W.; Choi, S.-H.; Kim, K.; Jin, J.-I. *J. Mater. Chem.* **2003**, *13*, 1900.
- (19) Peng, Z.; Bao, Z.; Galvin, M. E. *Chem. Mater.* **1998**, *10*, 2086.
- (20) Chen, Z.-K.; Meng, H.; Lai, Y.-H.; Huang, W. *Macromolecules* **1999**, *32*, 4351.
- (21) Wang, C.; Kilitziraki, M.; Palsson, L.-O.; Bryce, M. R.; Monkman, A. P.; Samuel, I. D. W. *Adv. Funct. Mater.* **2001**, *11*, 47.
- (22) Sung, H. H.; Lin, H. C. *Macromolecules* **2004**, *37*, 7945.

- (23) Wu, F. I.; Reddy, D. S.; Shu, C. F.; Liu, M. S.; Jen, A. K. Y. *Chem. Mater.* **2003**, *15*, 269.
- (24) (a) Wang, P.; Chai, C. P.; Chuai, Y. T.; Wang, F. Z.; Chen, X. F.; Fan, X. H.; Xu, Y. D.; Zou, D. C.; Zhou, Q. F. *Polymer* **2007**, *48*, 5889. (b) Wang, P.; Chai, C. P.; Yang, Q.; Wang, F. Z.; Shen, Z.; Guo, H. Q.; Chen, X. F.; Fan, X. H.; Zou, D. C.; Zhou, Q. F. *J. Polym. Sci., Part A: Polym. Chem.* **2008**, *46*, 5452.
- (25) Chai, C. P.; Zhu, X. Q.; Wang, P.; Ren, M. Q.; Chen, X. F.; Xu, Y. D.; Fan, X. H.; Ye, C.; Chen, E. Q.; Zhou, Q. F. *Macromolecules* **2007**, *40*, 9361.
- (26) Brandsma, L.; Vasilevsky, S. F.; Verkruijsse, H. D. *Application of Transition Metal Catalysts in Organic Synthesis*, corrected ed.; Springer: Berlin, 1999; p 5.
- (27) Chai, C. P.; Yang, Q.; Fan, X. H.; Chen, X. F.; Shen, Z.; Zhou, Q. F. *Liq. Cryst.* **2008**, *35*, 133.
- (28) Cho, H.-J.; Hwang, D.-H.; Lee, J.-I.; Jung, Y.-K.; Park, J.-H.; Lee, J.; Lee, S.-K.; Shim, H.-K. *Chem. Mater.* **2006**, *18*, 3780.
- (29) Hsieh, B. Y.; Chen, Y. *Macromolecules* **2007**, *40*, 8913.
- (30) Neher, D. *Macromol. Rapid Commun.* **2001**, *22*, 1365.
- (31) (a) Morgado, J.; Cacialli, F.; Friend, R. H.; Iqbal, R.; Yahioglu, G.; Milgrom, L. R.; Moratti, S. C.; Holmes, A. B. *Chem. Phys. Lett.* **2000**, *325*, 552. (b) Tang, C. W.; VanSlyke, S. A.; Chen, C. H. *J. Appl. Phys.* **1989**, *65*, 3610.
- (32) Wu, C. W.; Tsai, C. M.; Lin, H. C. *Macromolecules* **2006**, *39*, 4298.

MA802414S